

RAMS - Regional Atmospheric Modeling System

Department of Atmospheric Science, Colorado State University
and
ASTeR Division of Mission Research Corporation

Rosie Polkinghorne

ATOC 7500 - Meteorological Mesoscale Modeling

4/25/08

Non-hydrostatic, compressible equations

Equations of motion:

$$\begin{aligned}\frac{\partial u}{\partial t} &= -u \frac{\partial u}{\partial x} - v \frac{\partial u}{\partial y} - w \frac{\partial u}{\partial z} - \theta \frac{\partial \pi'}{\partial x} + fv + \frac{\partial}{\partial x} \left(K_m \frac{\partial u}{\partial x} \right) + \frac{\partial}{\partial y} \left(K_m \frac{\partial u}{\partial y} \right) + \frac{\partial}{\partial z} \left(K_m \frac{\partial u}{\partial z} \right) \\ \frac{\partial v}{\partial t} &= -u \frac{\partial v}{\partial x} - v \frac{\partial v}{\partial y} - w \frac{\partial v}{\partial z} - \theta \frac{\partial \pi'}{\partial y} + fu + \frac{\partial}{\partial x} \left(K_m \frac{\partial v}{\partial x} \right) + \frac{\partial}{\partial y} \left(K_m \frac{\partial v}{\partial y} \right) + \frac{\partial}{\partial z} \left(K_m \frac{\partial v}{\partial z} \right) \\ \frac{\partial w}{\partial t} &= -u \frac{\partial w}{\partial x} - v \frac{\partial w}{\partial y} - w \frac{\partial w}{\partial z} - \theta \frac{\partial \pi'}{\partial z} - g \frac{\theta'}{\theta_0} + \frac{\partial}{\partial x} \left(K_m \frac{\partial w}{\partial x} \right) + \frac{\partial}{\partial y} \left(K_m \frac{\partial w}{\partial y} \right) + \frac{\partial}{\partial z} \left(K_m \frac{\partial w}{\partial z} \right)\end{aligned}$$

Thermodynamic equation:

$$\frac{\partial \theta_{il}}{\partial t} = -u \frac{\partial \theta_{il}}{\partial x} - v \frac{\partial \theta_{il}}{\partial y} - w \frac{\partial \theta_{il}}{\partial z} + \frac{\partial}{\partial x} \left(K_h \frac{\partial \theta_{il}}{\partial x} \right) + \frac{\partial}{\partial y} \left(K_h \frac{\partial \theta_{il}}{\partial y} \right) + \frac{\partial}{\partial z} \left(K_h \frac{\partial \theta_{il}}{\partial z} \right) + \left(\frac{\partial \theta_{il}}{\partial t} \right)_{rad}$$

Water species mixing ratio continuity equation:

$$\frac{\partial r_n}{\partial t} = -u \frac{\partial r_n}{\partial x} - v \frac{\partial r_n}{\partial y} - w \frac{\partial r_n}{\partial z} + \frac{\partial}{\partial x} \left(K_h \frac{\partial r_n}{\partial x} \right) + \frac{\partial}{\partial y} \left(K_h \frac{\partial r_n}{\partial y} \right) + \frac{\partial}{\partial z} \left(K_h \frac{\partial r_n}{\partial z} \right)$$

Mass continuity equation:

$$\frac{\partial \pi'}{\partial t} = \frac{R\pi_0}{c_v \rho_0 \theta_0} \left(\frac{\partial \rho_0 \theta_0 u}{\partial x} + \frac{\partial \rho_0 \theta_0 v}{\partial y} + \frac{\partial \rho_0 \theta_0 w}{\partial z} \right)$$

Exner function

$$\pi = C_p (p / p_0)^{R/C_p} = C_p T_v / \theta$$

- The pressure perturbation term does not occur in the gravity term
- Removes the need to compute the density perturbation - one less equation
- The vertical gradient of π is much less than that of p , introducing less error when using finite difference techniques

A few details

- 2-D or 3-D
- Staggered Arakawa-C grid - all thermodynamic and moisture variables are defined at the same point, with the velocity components u , v , and w defined at $1/2 \Delta x$, $1/2 \Delta y$, and $1/2 \Delta z$, respectively
- Vertical grid spacing can be stretched
- Unlimited number of nested grids, grids can be added/removed during the simulation, grids can be moved during the simulation
- No minimum horizontal or vertical resolution
- No lower size limit on a limited-area model domain, may be run on a global domain

Initialization

- Horizontally homogeneous from a single sounding
- RAMS/ISAN package
 - Horizontal wind components, pressure, and relative humidity from the gridded global analysis and any available rawinsonde data are interpolated vertically to isentropic levels at a user-specified resolution.
 - The Barnes objective analysis scheme is applied on the isentropic surfaces
 - The isentropic dataset is then transferred to the model grid using overlapping polynomial interpolation

Advantages to the RAMS/ISAN package

- An objective analysis better approximates the interstation variability of the atmospheric fields since synoptic flow is roughly adiabatic
- Isentropes tend to be packed in frontal areas, providing enhanced resolution along discontinuities
- Short-wavelength features in Cartesian coordinates are transformed in the isentropic system into longer-wavelength features that can be more accurately analyzed objectively with much less smoothing than with other coordinate systems

Disadvantages to the RAMS/ISAN package

- The vertical resolution decreases as the atmospheric stability increases
- Isentropes frequently intersect the ground
 - a “hybrid” vertical coordinate is included, a mixture of isentropic and terrain following coordinates

Solution Technique

- Velocity components and Exner function marched forward with leapfrog time differencing
- All scalar quantities other than the Exner function use forward-upstream time differencing
- Time-splitting is used to step forward the acoustic terms

Leapfrog phase and amplitude errors - advection

Amplitude

	0.001	0.01	0.1	0.2	0.3	0.4	0.5	0.6	0.7	0.8	0.9	1.0
$2\Delta x$	1.000	1.000	1.000	1.000	1.000	1.000	1.000	1.000	1.000	1.000	1.000	1.000
$4\Delta x$	1.000	1.000	1.000	1.000	1.000	1.000	1.000	1.000	1.000	1.000	1.000	1.000
$10\Delta x$	1.000	1.000	1.000	1.000	1.000	1.000	1.000	1.000	1.000	1.000	1.000	1.000
$20\Delta x$	1.000	1.000	1.000	1.000	1.000	1.000	1.000	1.000	1.000	1.000	1.000	1.000

Phase

	0.001	0.01	0.1	0.2	0.3	0.4	0.5	0.6	0.7	0.8	0.9	1.0
$2\Delta x$	0.000	0.000	0.000	0.000	0.000	0.000	0.000	0.000	0.000	0.000	0.000	0.000
$4\Delta x$	0.637	0.637	0.638	0.641	0.647	0.655	0.667	0.683	0.705	0.738	0.791	1.000
$10\Delta x$	0.935	0.935	0.936	0.938	0.940	0.944	0.950	0.956	0.964	0.974	0.986	1.000
$20\Delta x$	0.984	0.984	0.984	0.984	0.985	0.986	0.988	0.989	0.991	0.994	0.997	1.000

Data from Pielke (2001)

Forward amplitude errors - advection

TABLE 1. Amplification factor for the advective form and constant grid flux form.

Order	Courant number						
	0.01	0.1	0.3	0.5	0.7	0.9	1.0
$2\Delta x$							
1	0.980	0.800	0.400	0.000	0.400	0.800	1.000
2	1.000	0.980	0.820	0.500	0.020	0.620	1.000
3	0.986	0.848	0.456	0.000	0.456	0.848	1.000
4	1.000	0.973	0.765	0.375	0.147	0.723	1.000
5	0.989	0.868	0.481	0.000	0.481	0.868	1.000
6	1.000	0.970	0.737	0.313	0.225	0.766	1.000
7	0.991	0.880	0.495	0.000	0.495	0.880	1.000
8	1.000	0.968	0.719	0.273	0.272	0.792	1.000
9	0.992	0.888	0.505	0.000	0.505	0.888	1.000
10	1.000	0.966	0.706	0.246	0.305	0.809	1.000
$4\Delta x$							
1	0.990	0.906	0.762	0.707	0.762	0.906	1.000
2	1.000	0.995	0.958	0.901	0.866	0.920	1.000
3	0.997	0.966	0.908	0.884	0.908	0.966	1.000
4	1.000	0.997	0.978	0.952	0.943	0.971	1.000
5	0.999	0.986	0.961	0.950	0.961	0.986	1.000
6	1.000	0.999	0.989	0.978	0.975	0.988	1.000
7	0.999	0.994	0.983	0.978	0.983	0.994	1.000
8	1.000	0.999	0.995	0.990	0.989	0.995	1.000
9	1.000	0.997	0.992	0.989	0.992	0.997	1.000
10	1.000	1.000	0.998	0.995	0.995	0.998	1.000
$8\Delta x$							
1	0.997	0.973	0.936	0.924	0.936	0.973	1.000
2	1.000	1.000	0.996	0.992	0.989	0.993	1.000
3	1.000	0.997	0.993	0.992	0.993	0.997	1.000
4	1.000	1.000	1.000	0.999	0.999	0.999	1.000
5	1.000	1.000	0.999	0.999	0.999	0.999	1.000
6	1.000	1.000	1.000	1.000	1.000	1.000	1.000
7	1.000	1.000	1.000	1.000	1.000	1.000	1.000
8	1.000	1.000	1.000	1.000	1.000	1.000	1.000
9	1.000	1.000	1.000	1.000	1.000	1.000	1.000
10	1.000	1.000	1.000	1.000	1.000	1.000	1.000

From Tremback et al (1987)

Forward phase errors - advection

- 6th order scheme seems to have the best balance between accuracy and efficiency
- The cost of a 6th order scheme is not prohibitive and errors are significantly smaller than lower-order schemes

TABLE 2. Phase speed ratio for the advective form and constant grid flux form.

Order	Courant number						
	0.01	0.1	0.3	0.5	0.7	0.9	1.0
$4\Delta x$							
1	0.643	0.704	0.859	1.000	1.060	1.033	1.000
2	0.637	0.641	0.676	0.749	0.856	0.964	1.000
3	0.852	0.879	0.945	1.000	1.023	1.013	1.000
4	0.849	0.852	0.873	0.911	0.956	0.991	1.000
5	0.935	0.947	0.976	1.000	1.010	1.006	1.000
6	0.934	0.935	0.946	0.964	0.983	0.997	1.000
7	0.971	0.976	0.989	1.000	1.005	1.003	1.000
8	0.970	0.971	0.976	0.984	0.993	0.999	1.000
9	0.986	0.989	0.995	1.000	1.002	1.001	1.000
10	0.986	0.987	0.989	0.993	0.997	1.000	1.000
$8\Delta x$							
1	0.903	0.926	0.970	1.000	1.013	1.008	1.000
2	0.900	0.901	0.910	0.928	0.953	0.984	1.000
3	0.989	0.991	0.996	1.000	1.002	1.000	1.000
4	0.988	0.988	0.990	0.992	0.995	0.999	1.000
5	0.999	0.999	1.000	1.000	1.000	1.000	1.000
6	0.999	0.999	0.999	0.999	0.999	1.000	1.000
7	1.000	1.000	1.000	1.000	1.000	1.000	1.000
8	1.000	1.000	1.000	1.000	1.000	1.000	1.000
9	1.000	1.000	1.000	1.000	1.000	1.000	1.000
10	1.000	1.000	1.000	1.000	1.000	1.000	1.000

From Tremback et al (1987)

Effective Resolution

Based on the phase and amplitude errors for both the forward and leapfrog schemes, the effective resolution of RAMS appears to be about $8\Delta x$

If a 6th-order forward scheme were used, the effective resolution could be increased to $4\Delta x$

Coordinate System

- Horizontal:
 - Cartesian
 - Polar stereographic
- Vertical:
 - Terrain-following σ_z

Terrain-Following σ_z

The top of the model domain is exactly flat and the bottom follows the terrain

$$x^* = x$$

$$y^* = y$$

$$z^* = H \left(\frac{z - z_g}{H - z_g} \right)$$

Lateral Boundary Condition

- Radiative condition

$$\frac{\partial u}{\partial t} = -(u + c) \frac{\partial u}{\partial x}$$

- Large-scale nudging
- Cyclic boundaries

Radiative Condition

- Orlanski (1976)

$$c = \frac{-\partial u}{\partial t} \Big/ \frac{\partial u}{\partial x}$$

- Klemp and Lilly (1978) - Orlanski phase velocities averaged in the vertical, then the average velocity applied to the whole column
- Klemp and Wilhelmson (1978) - phase velocity specified for a typical gravity wave

Klemp and Wilhelmson (1978)

- A value of $c=30$ m/s was tested, along with $c=10$ m/s and $c=50$ m/s
- Results compared against a reference simulation where the model domain is increased by a factor of 4
- They concluded that the simulation with $c=30$ m/s compares favorably with the reference simulation, although a smaller value of c might be a little better
- This boundary condition is used in my experiments with $c=20$ m/s

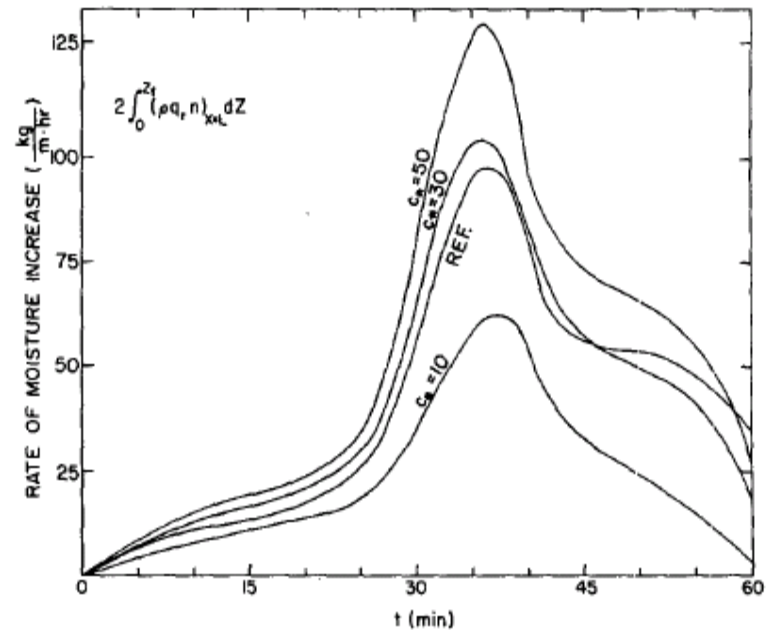


FIG. 10. Net moisture flux through the lateral boundaries for two-dimensional simulations as a function of c_* .

From Klemp and Wilhelmson (1978)

Klemp and Wilhelmson vs Orlanski

- Tripoli and Cotton (1982) tested the sensitivity of a 2-D simulation of a thunderstorm to these two boundary conditions
- For that case, the Orlanski boundary conditions are superior to Klemp and Wilhelmson
- These results agree with the experiments done by Clark (1979)

Top boundary condition

- Rigid lid
- Rigid lid with a high-viscosity layer aloft to damp gravity waves, by nudging to large-scale analysis or initial conditions

Subgrid Mixing Parameterization

- Smagorinsky (1963) deformation-K closure scheme
- Deardorff level 2.5 K - Eddy viscosity is a function of prognostic TKE (Deardorff, 1980)
- Mellor-Yamada level 2.5 - ensemble-averaged TKE (Mellor and Yamada, 1982)

Mellor-Yamada level 2.5

Inputs:

wind

potential temperature

turbulent kinetic energy

Outputs:

subgrid-scale fluxes

Cumulus Parameterization

Modified Kuo - convection acts to consume the convective instability generated by larger scales

Inputs:

environmental potential temperature

vertical velocity

total water

Outputs:

cloud top, LCL

profiles of heating and moistening

convective tendency terms for potential and total water

Radiation Parameterization

- Mahrer and Pielke (1977) long/shortwave model - no cloud processes
- Chen and Cotton (1983) long/shortwave model - cloud processes considering all condensate as liquid
- Harrington (1997) long/shortwave model - two-stream scheme interacts with liquid and ice hydrometeor size-spectra

Harrington (1997) long/shortwave model

- Transfer equations are solved for three model gases - H_2O , CO_2 , and O_3
- Optical properties of water droplets are computed using Lorenz-Mie theory, while the theories of Mitchell and Arnott (1994) and Mitchell et al (1996) are used to compute the optical properties of non-spherical ice crystals
- Rayleigh scatter and absorption are treated as independent of wavelength across a given band
- Scattering properties are calculated based on an assumed gamma distribution

Harrington (1997) long/shortwave model

Inputs:

model gas concentrations (H_2O , CO_2 , and O_3)
hydrometeor mixing ratios and size
distribution

Outputs:

long/shortwave radiative fluxes

Stable precipitation parameterization

- No cloud
- Condensation only
- Single-moment bulk scheme (Walko et al, 1995) - prognose mixing ratio
- Two-moment bulk scheme (Meyers et al, 1997) - prognose mixing ratio and number concentration

Two-moment bulk scheme (Meyers et al, 1997)

- Water is categorized as vapor, cloud droplets, rain, pristine ice, snow, hail, aggregates, and graupel
- Hydrometeors in each category are assumed to conform to a prescribed gamma distribution
- The conservation equation for hydrometeors includes advective and turbulent transport by the resolved and subgrid velocities in the model, sources and sinks which consist of all types of conversion from one category to another, and local losses and gains due to gravitational sedimentation

Two-moment bulk scheme (Meyers et al, 1997)

Inputs:

atmospheric pressure

atmospheric temperature

hydrometeor mixing ratio

hydrometeor number concentration

Outputs:

hydrometeor mixing ratio

hydrometeor number concentration

Computer aspects

- Parallel processing on distributed and shared memory platforms using Message Passing Interface (MPI)
- Originally run on mainframe computers such as CRAY and CYBER machines
- Now can be run on UNIX, LINUX, MS Windows 95/98/NT/2000
- Currently run on Lightning, an NCAR supercomputer running LINUX